The Astrophysical Journal, 670: L81–L84, 2007 December 1

NEW RESULTS ON PARTICLE ACCELERATION IN THE CENTAURUS A JET AND COUNTERJET FROM A DEEP *CHANDRA* OBSERVATION

M. J. Hardcastle,[1] R. P. Kraft,[2] G. R. Sivakoff,[3] J. L. Goodger,[1] J. H. Croston,[1] A. Jordán,[2,4] D. A. Evans,[2] D. M. Worrall,[2,5] M. Birkinshaw,[2,5] S. Raychaudhury,[2,6] N. J. Brassington,[2] W. R. Forman,[2] W. E. Harris,[7] C. Jones,[2] A. M. Juett,[8] S. S. Murray,[2] P. E. J. Nulsen,[2] C. L. Sarazin,[8] and K. A. Woodley[7]

Received 2007 September 6; accepted 2007 October 5; published 2007 October 29

ABSTRACT

We present new deep *Chandra* observations of the Centaurus A jet, with a combined on-source exposure time of 719 ks. These data allow detailed X-ray spectral measurements to be made along the jet out to its disappearance at 4.5 kpc from the nucleus. We distinguish several regimes of high-energy particle acceleration; while the inner part of the jet is dominated by knots and has properties consistent with local particle acceleration at shocks, the particle acceleration in the outer 3.4 kpc of the jet is likely to be dominated by an unknown distributed acceleration mechanism. In addition to several compact counterjet features, we detect probable extended emission from a counterjet out to 2.0 kpc from the nucleus and argue that this implies that the diffuse acceleration process operates in the counterjet as well. A preliminary search for X-ray variability finds no jet knots with dramatic flux density variations, unlike the situation seen in M87.

Subject headings: galaxies: active — galaxies: individual (Centaurus A) — galaxies: jets — X-rays: galaxies

1. INTRODUCTION

Low-power, Fanaroff-Riley class I (FR I; Fanaroff & Riley 1974) radio galaxies are numerically the dominant population of radio-loud active galaxies in the universe. Their dynamics and energy content are thus essential to models of AGN "feedback" in which the energy released in the process of accretion onto the central supermassive black hole is transported to large spatial scales via the interaction between the jets and the external medium. To understand the dynamics and energetics of these sources it is crucial that we understand the particle acceleration processes by which the bulk kinetic energy of the jets is translated into the internal energy of relativistic plasma.

The discovery with *Chandra* that X-ray emission is common in the inner few kiloparsecs of FR I jets (Worrall et al. 2001) provides a very strong argument that in situ high-energy particle acceleration is taking place in those regions. The broadband spectral energy distribution and X-ray spectrum of the X-ray emission imply a synchrotron origin for the X-rays (Hardcastle et al. 2001). For magnetic fields close to the equipartition value in a typical powerful jet, the loss timescale ($\tau = -E/\dot{E}$) for the $\gamma \sim 10^7$–10^8 electrons emitting X-ray synchrotron emission is tens of years. Thus, observations of X-ray synchrotron emission essentially tell us where particle acceleration is happening *now*; in particular, resolved, diffuse X-ray emission implies a particle acceleration mechanism that must be distributed throughout the jet.

To probe the nature of the acceleration mechanisms in FR I jets we require observations that can reliably distinguish between compact and diffuse X-ray emission; this implies (at the most optimistic) a spatial resolution that is comparable to the loss spatial scale, the distance traveled by an electron before synchrotron losses remove it from the X-ray band, or roughly $c\tau$. Even with the comparatively high angular resolution of *Chandra*, this can only be achieved in the nearest FR I radio galaxy, Centaurus A. Given Cen A's distance of ~3.7 Mpc (the average of five distance estimates to Cen A; Ferrarese et al. 2007), *Chandra*'s resolution corresponds to ~10 pc.

Chandra observations of Cen A show a complex, knotty, and in places edge-brightened jet structure (Kraft et al. 2000, 2002; Hardcastle et al. 2003, hereafter H03; Kataoka et al. 2006, hereafter K06; Hardcastle et al. 2006, hereafter H06). It has been argued (H03, K06) that at least two acceleration mechanisms are required; the dynamics and spectra of the compact knots in the inner part of the jet are consistent with a shock origin, while the diffuse emission is inconsistent both spectrally (H03) and in terms of the number distribution of knots (K06) with being the sum of many unresolved knots with the same properties as those observed and is instead probably truly diffuse, implying a distributed acceleration mechanism such as second-order Fermi acceleration (e.g., Stawarz & Ostrowski 2002) or magnetic field line reconnection (e.g., Birk & Lesch 2000). Here we present the results of new, much deeper *Chandra* observations and their consequences for the nature of particle acceleration in the Cen A jet and counterjet.

In this analysis *Chandra* data processing was done using CIAO version 3.4 and CALDB version 3.3.0.1. Spectral fitting was carried out in XSPEC. We define the spectral index α such that flux $\propto \nu^{-\alpha}$; the photon index $\Gamma = 1 + \alpha$. Errors quoted and plotted throughout are 1 σ for one interesting parameter.

2. OBSERVATIONS

The *Chandra* AXAF CCD Imaging Spectrometer (ACIS) has observed Cen A four times prior to 2007 (ObsIDs 316, 962, 2978, and 3965) for a total of 157 ks (see, e.g., Kraft et

[1] School of Physics, Astronomy and Mathematics, University of Hertfordshire, College Lane, Hatfield AL10 9AB, UK; m.j.hardcastle@herts.ac.uk, j.l.goodger@herts.ac.uk, j.h.croston@herts.ac.uk.

[2] Harvard-Smithsonian Center for Astrophysics, 60 Garden Street, Cambridge, MA 02138; kraft@head.cfa.harvard.edu, ajordan@cfa.harvard.edu, devans@cfa.harvard.edu, nbrassington@cfa.harvard.edu, wforman@cfa.harvard.edu, cjones@cfa.harvard.edu, ssm@cfa.harvard.edu, pnulsen@cfa.harvard.edu.

[3] Department of Astronomy, The Ohio State University, 4055 McPherson Laboratory 140 W. 18th Avenue, Columbus, OH 43210-1173; sivakoff@astronomy.ohio-state.edu.

[4] European Southern Observatory, Karl-Schwarzschild-Strasse 2, 85748 Garching bei München, Germany.

[5] Department of Physics, University of Bristol, Tyndall Avenue, Bristol BS8 ITL, UK; d.m.worrall@bristol.ac.uk, mark.birkinshaw@bristol.ac.uk.

[6] School of Physics and Astronomy, University of Birmingham, Edgbaston, Birmingham B15 2TT, UK; somak@star.sr.bham.ac.uk.

[7] Department of Physics and Astronomy, McMaster University, Hamilton, ON L8S 4M1, Canada; harris@physics.mcmaster.ca, woodleka@physics.mcmaster.ca.

[8] Department of Astronomy, University of Virginia, P. O. Box 400325, Charlottesville, VA 22904-4325; ajuett@virginia.edu, sarazin@virginia.edu.

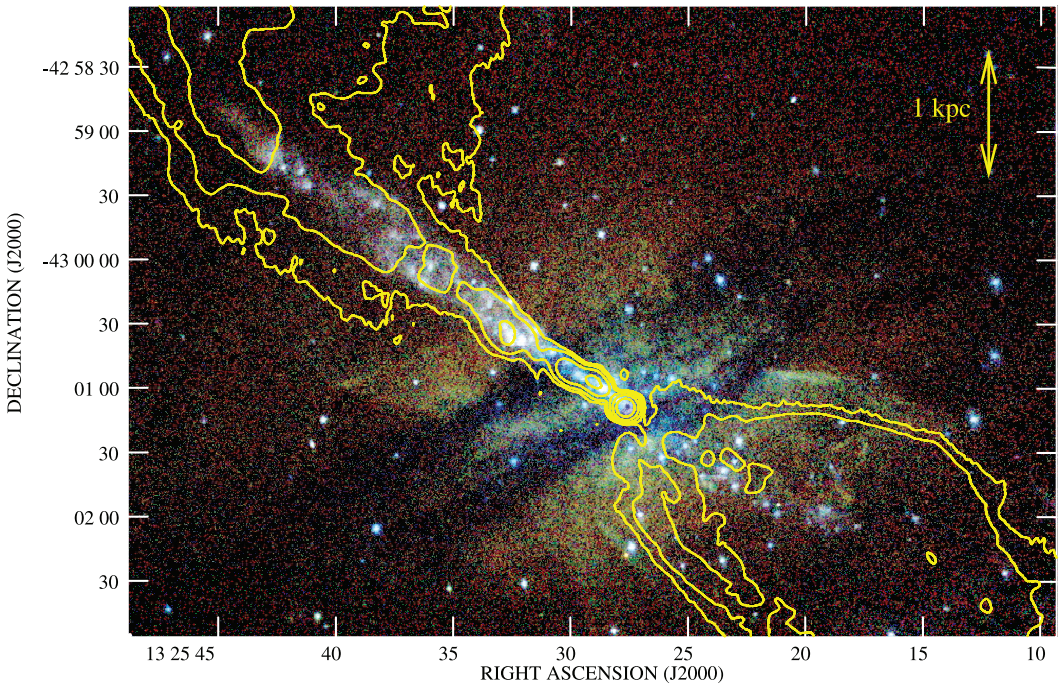

FIG. 1.—False-color image of the jet and counterjet regions of Cen A using all ACIS observations. The *Chandra* data from each observation have been exposure-corrected at an appropriate energy and then combined, weighting according to the value of the exposure map. The images are binned in standard *Chandra* pixels (0.492″ on a side) and smoothed with a FWHM = 1.0″ Gaussian. Red shows exposure-corrected counts in the energy range 0.4–0.85 keV, green shows 0.85–1.3 keV, and blue 1.3–2.5 keV. Contours [7 × (1, 4, 16, …) mJy beam^{-1}] are from the 5 GHz VLA map of H06 with 6.0″ resolution.

al. 2002; H03; K06) and six additional times in 2007 for the Cen A Very Large Project (Cen A-VLP; ObsIDs 7797, 7798, 7799, 7800, 8489, and 8490). The combined ACIS data set has an effective on-source time of 719 ks. All X-ray spectral fits are the result of joint fitting to spectra extracted from matching regions from each separate observation. Figure 1 shows a false-color image of the jet and counterjet region.

Cen A has also been extensively observed in the radio using the NRAO Very Large Array (VLA). In this Letter we make use of radio data whose reduction was described by H03 and H06. We also use new observations at 8.4 GHz taken on 2007 June 04 (observation AG754) as part of our ongoing program to monitor proper motions and variability in the Cen A radio jet. These data and the results of the monitoring program will be presented elsewhere (J. L. Goodger et al., in preparation). For radio/X-ray comparisons, we have aligned both the radio and X-ray frames to the VLBI position of the nucleus quoted by Ma et al. (1998). The relative astrometric alignment of the *Chandra* data was done in the manner described by Jordán et al. (2007). We then determined the X-ray centroid of the nucleus by two independent methods (determining the intersection of the readout streaks and centroiding on the hard wings of the AGN PSF), which gave consistent results. The resulting radio/X-ray alignment is accurate to $\pm 0.1''$.

Figure 1 shows a number of interesting features of the new deep *Chandra* observation. The jet is now detected with high signal-to-noise ratio out to 250″ (4.5 kpc in projection) from the active nucleus, and this allows us to extract spectra for a large number of jet regions; we discuss the jet spectra in § 3. Diffuse emission plausibly related to a counterjet is now detected out to 110″ (2.0 kpc); we discuss the nature of this emission and its implications in § 4. Constraints on large-scale variability in jet knots are discussed in § 5.

3. SPECTRA OF DIFFUSE AND COMPACT FEATURES

To investigate the jet X-ray spectrum we followed K06 in dividing the jet into compact and diffuse regions. We defined as a knot any compact feature in the jet that is clearly distinguished (by a factor $\gtrsim 2$) in surface brightness from its surroundings and has a radius $<2''$. These criteria include many, but not all, of the knots discussed by Kraft et al. (2002) and K06; by our definition there are 26 knots in the jet, all but four of which are bright enough for spectral analysis. We extracted spectra for these knots using the PSEXTRACT script, fitting a power-law spectrum with a single normalization and photon index and with absorption that was free to vary above the Galactic value (we adopt $N_{\rm H} = 8.4 \times 10^{20}$ cm^{-2}, as reported by the COLDEN code; Dickey & Lockman 1990) but constrained not to fall below it. The effects of knot variability on this fitting are discussed in § 5. Background subtraction was done using local off-source background regions, taking into account the variation in both background surface brightness and column density. The knot spectra may therefore include a small amount of contamination from diffuse jet background.

The diffuse region of the jet was taken to be a polygonal region including all jet-related emission but excluding all features defined above as knots. We divided this region into rectangular subregions whose long axes were the whole transverse width of the jet (transverse spectral variations in the jet are discussed by Worrall et al. 2007) and whose short axes were allowed to grow in a direction parallel to the jet axis, in steps of 1 *Chandra* pixel, until sufficient counts were enclosed in all regions for spectroscopic analysis ($\gtrsim 1000$ counts in the combined data set before background subtraction). This process gave a total of 53 extended regions. Spectra for these regions were extracted with the SPECEXTRACT script and were fitted

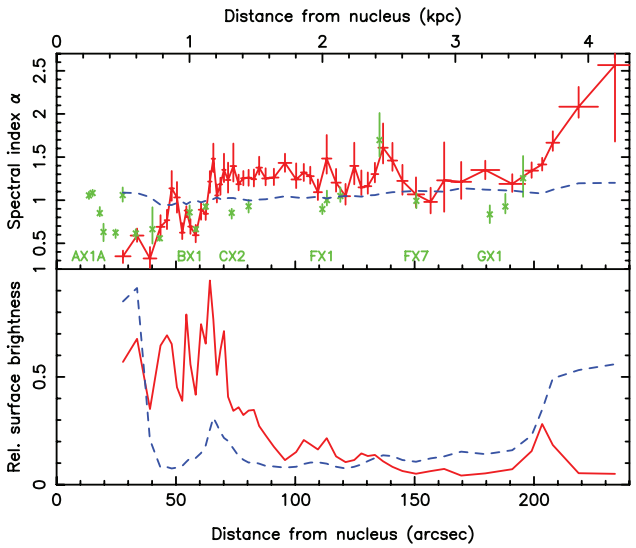

FIG. 2.—Spectral index and surface brightness in the jet of Cen A. *Top*: Red line shows the spectral index in the extended regions (α_X); the dashed blue line shows the radio/X-ray two-point spectral index, α_{RX}, for extended emission. Green stars show the positions and X-ray spectral indices of knots. Vertical bars are 1 σ errors; horizontal bars show the size of extended extraction regions. *Bottom*: Surface brightness profile (arbitrary units) for extended emission in X-ray (*red solid line*) and radio (*blue dashed line*).

with absorbed power-law models in precisely the same manner as the knots. All the fits for knots and extended regions were acceptable (probability under the null hypothesis >2%).

The results of this process are summarized in Figure 2, which may be compared with Figure 4 of K06 and Table 2 of H03. Based on this profile, the extended emission of the jet can be divided into three regions with different radio and X-ray properties:

1. $\theta < 60''$, *except at* $\theta \approx 50''$.—X-ray flux dominated by knots ($\sim\frac{2}{3}$ of total flux in knots; H03); radio surface brightness high; extended α_X flat, often flatter than α_{RX}, and comparable to α_X of knots.
2. $\theta \approx 50''$ *and* $60'' < \theta < 190''$.—Few X-ray knots (<10% of flux in knots); knots have α_X less than the extended value. $\alpha_X > \alpha_{RX}$ and roughly constant, $\approx 1.2 \pm 0.2$. Radio surface brightness low, increasing by a factor of ~2 along the jet. X-ray surface brightness flat but decreasing by a factor of ~2 along the jet. Edge-brightening along the jet present in the X-ray.
3. $\theta > 190''$, *at and beyond the "flare point" of H06*.—α_X steepens to very high values, ~2.5. Radio surface brightness increases by factor of ~3. X-ray surface brightness increases by factor of ~3, then falls off to zero.

In region 1, the flat X-ray spectral index of the extended emission is consistent with the expectations from shock acceleration coupled with rapid downstream expansion losses (although some of the inner knots have well-determined steep spectra, possibly implying higher magnetic fields in these regions), while the fact that $\alpha_{RX} > \alpha_X$ is inconsistent with a one-zone model, but is consistent with the idea that much of the particle acceleration here is localized to small subregions of the jet. The new data provide some evidence that structures that appeared diffuse in earlier observations (e.g., around knot B) are in fact composed of smaller subclumps. In region 2, on the other hand, the X-ray and radio/X-ray spectral indices and the general appearance of the jet—dominated not by knots but

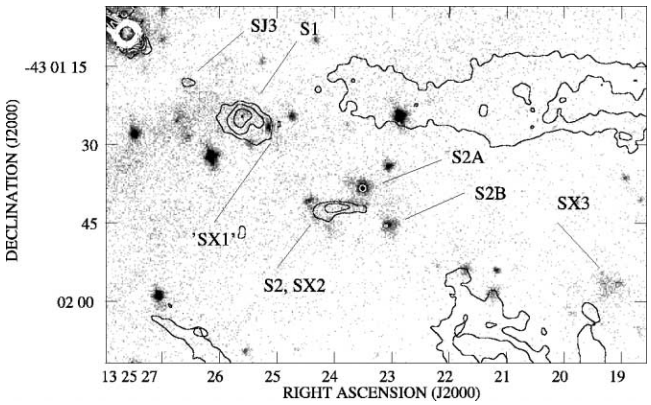

FIG. 3.—Counterjet region of Cen A. Gray scale shows accumulated raw counts in the *Chandra* observations in the 0.4–2.5 keV energy band, binned in 0.246″ pixels. Contours [0.1 × (1, 2, 4, …) mJy beam^{-1}] are from the 8.4 GHz A+B-configuration VLA map of H03, smoothed to a resolution of 1.5″. The radio data are only sensitive to features on scales $\lesssim$20″.

by filamentary, sometimes edge-brightened features—are consistent with a truly diffuse acceleration mechanism, as argued by K06. Finally, as discussed by H06, region 3 corresponds to the end of X-ray emission from the jet. The remarkable X-ray spectral steepening in this region cannot be due to synchrotron losses—the spatial scales involved are too large—but must be due to a progressive loss of efficiency of high-energy particle acceleration. H06 showed that the mid-IR and radio data are consistent with the idea that there is no particle acceleration beyond the end of the X-ray emission at ~240″; the new data provide additional evidence that whatever happens at the "flare point"—perhaps a significant jet deceleration—makes the diffuse acceleration process substantially less efficient at producing high-energy electrons. Our ability to distinguish between the different models for the distributed particle acceleration process (§ 1) is limited by the inability of these models to produce detailed predictions for the particle energy spectrum, but the steep spectra seen at the end of the Cen A jet represent a challenge for any current model.

4. THE COUNTERJET

H03 showed that a number of X-ray features in the counterjet region had radio counterparts, proving that a coherent counterjet does exist on the kiloparsec scale in Cen A, although no large-scale radio emission is detected from it. With the new X-ray data we detect at least four more counterjet features (Fig. 3). There is now a weak X-ray counterpart to the compact radio knot SJ3 (using the notation of H03) and to the diffuse feature S1. The feature denoted SX1 by H03, with no radio counterpart, turns out to be strongly variable (see § 5) and so may be unrelated to the counterjet. However, the two radio knots S2A and S2B have very clear X-ray counterparts with stable X-ray fluxes. There is also a clear overdensity of fainter compact X-ray features, some of which may be counterjet knots, although none has a radio counterpart. The most striking new counterjet features are the *extended* features SX2 and SX3, the former of which has a curious V-shaped morphology with a radio counterpart to one arm of the V, and the latter of which appears as a patch of diffuse emission on scales of 13″ (230 pc). Both of these have clearly harder spectra than the surrounding thermal emission or than other nearby filamentary structures in the lobe region (Fig. 1). We extracted spectra for these regions from the 2007 data sets only, obtaining a good fit with power-law models with free ab-

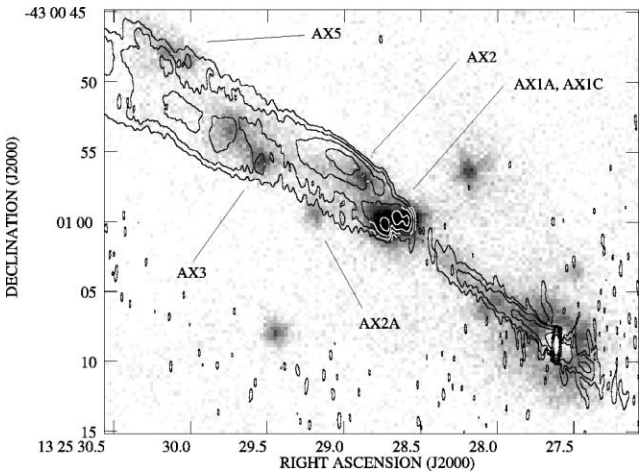

FIG. 4.—Inner jet of Cen A. Gray scale as in Fig. 3. Contours [0.15 × (1, 4, 16, …) mJy beam^{-1}] are from the 8.4 GHz A-configuration VLA data taken in 2007, with a resolution of 0.84″ × 0.22″.

sorption as for the other spectra, and found $\alpha_X = 1.42^{+0.21}_{-0.14}$ and $0.85^{+0.10}_{-0.15}$ for SX2 and SX3, respectively, consistent with the range of spectra seen for extended regions of the jet discussed in § 3, although we cannot rule out thermal models with $kT \gtrsim 3.5$ keV. SX3's 1 keV flux density of 2.3 ± 0.4 nJy would imply a 5 GHz flux density for a counterpart of ∼20 mJy, if it were similar to extended regions of the northern jet at comparable nuclear distances, which is hard to rule out given the strong filamentary structure in the S lobe. (For comparison, 5 GHz flux densities for S1 and S2 are ∼60 and ∼80 mJy, respectively.) SX3's similarity in the X-ray to the diffuse structure of jet features at a similar off-nuclear distance gives us the first evidence that the diffuse acceleration process can also operate in the counterjet. If this is so, it is unclear why only this one purely diffuse counterjet feature is visible in X-rays. The fact that the jet-counterjet ratio in the X-ray is, in general, higher for extended regions than for compact sources lends some support to the model in which X-ray–emitting knots are stationary while the diffuse emission comes from the bulk flow.

5. KNOT VARIABILITY AND FLARING

A goal of the Cen A-VLP was to search for extreme variability in jet knots such as that seen in knot HST-1 of M87 (e.g., Harris et al. 2006). Only two bright X-ray features related to the jets show very strong variability in the 10 epochs available. The counterjet feature SX1 appears to have flared in the 2003 observations (H03) when its 1 keV flux density is 9 ± 1 nJy compared to ∼2 nJy in all other observations. Its rather flat spectrum ($\alpha_X = 0.4 \pm 0.1$), the fact that it is unresolved, and the lack of a radio counterpart means that it may well be a low-mass X-ray binary (LMXB) unrelated to the counterjet. More interesting is the feature AX2A detected in the 2007 observations in the inner jet (Fig. 4). The 1 keV flux density of this feature is a constant 5 ± 1 nJy in 2007 and <1 nJy at all earlier times; it has $\alpha_X = 0.65 \pm 0.1$. As Figure 4 shows, it is just at the edge of the radio jet, is compact or unresolved, and has no detected radio counterpart; given its flux density, we might have expected one at the level of a few mJy if it were a jet knot. While continued monitoring of this feature will be interesting, it seems most likely that it too is an unrelated LMXB. There is thus no evidence for extreme variability in any bona fide jet knot in Cen A, consistent with the fact that many of the X-ray and radio knots are spatially resolved. Evidence for weaker variability in the X-ray and radio will be discussed in a future paper (J. L. Goodger et al., in preparation).

6. SUMMARY

The inner part of the Cen A jet is dominated by the shock-related knots discussed by H03, although we have so far failed to see the dramatic variability seen in M87, interpreted as large changes in particle acceleration processes or in jet flow. The radio-associated compact features in the counterjet are likely also the result of small-scale shocks, presumably caused as the counterjet flow encounters compact obstacles. However, the outer 3.4 kpc of the jet—and possibly also the newly detected extended X-ray counterjet components—are different from the shock-dominated regions in their X-ray spectra and structure and in their radio/X-ray ratio. Our results add to the evidence that an unknown, distributed particle acceleration process operates in the jet of Cen A. Diffuse X-ray emission with a similar broadband spectrum is seen in the jets of many other FR I sources (e.g., 3C 66B; Hardcastle et al. 2001), and it also resembles the extended synchrotron X-ray emission seen in the jets (e.g., K06) and hot spots (e.g., Hardcastle et al. 2007) of the more powerful FR IIs. The Cen A data allow us to study the spatial and spectral properties of this emission and the physical processes responsible for it in more detail than is possible in any other object.

We gratefully acknowledge financial support for this work from the Royal Society (research fellowship for M. J. H.), the STFC (reseach studentship for J. L. G.), and NASA (grant GO7-8105X to R. P. K.). The National Radio Astronomy Observatory is a facility of the National Science Foundation operated under cooperative agreement by Associated Universities, Inc.

Facilities: CXO(ACIS), VLA

REFERENCES

Birk, G. T., & Lesch, M. 2000, ApJ, 530, L77
Dickey, J. M., & Lockman, F. J. 1990, ARA&A, 28, 215
Fanaroff, B. L., & Riley, J. M. 1974, MNRAS, 167, 31P
Ferrarese, L., Mould, J. R., Stetson, P. B., Tonry, J. L., Blakeslee, J. P., & Ajhar, E. A. 2007, ApJ, 654, 186
Hardcastle, M. J., Birkinshaw, M., & Worrall, D. M. 2001, MNRAS, 326, 1499
Hardcastle, M. J., Croston, J. H., & Kraft, R. P. 2007, ApJ, 669, 893
Hardcastle, M. J., Kraft, R. P., & Worrall, D. M. 2006, MNRAS, 368, L15 (H06)
Hardcastle, M. J., Worrall, D. M., Kraft, R. P., Forman, W. R., Jones, C., & Murray, S. S. 2003, ApJ, 593, 169 (H03)
Harris, D. E., Cheung, C. C., Biretta, J. A., Sparks, W. B., Junor, W., Perlman, E. S., & Wilson, A. S. 2006, ApJ, 640, 211
Jordán, A., et al. 2007, ApJL, submitted
Kataoka, J., Stawarz, Ł., Aharonian, F., Takahara, F., Ostrowski, M., & Edwards, P. G. 2006, ApJ, 641, 158 (K06)
Kraft, R. P., Forman, W. R., Jones, C., Murray, S. S., Hardcastle, M. J., & Worrall, D. M. 2002, ApJ, 569, 54
Kraft, R. P., et al. 2000, ApJ, 531, L9
Ma, C., et al. 1998, AJ, 116, 516
Stawarz, Ł., & Ostrowski, M. 2002, ApJ, 578, 763
Worrall, D. M., Birkinshaw, M., & Hardcastle, M. J. 2001, MNRAS, 326, L7
Worrall, D. M., et al. 2007, ApJL, submitted